Received: 19 September 2023 | Revised: 19 October 2023 | Accepted: 1 November 2023

DOI: 10.1002/pol.20230704

RESEARCH ARTICLE

JOURNAL OF POLYMER SCIENCE WILEY

A unified approach for evaluating mechanical compression tests for polymer bead foams

Rodrigo Q. Albuquerque | **Johannes Meuchelböck** | **Holger Ruckdäschel**

University of Bayreuth, Bayreuth, Germany

Correspondence
Holger Ruckdäschel, University of Bayreuth, Universitätsstrasse 30, Bayreuth 95447, Germany.
Email: ruckdaeschel@uni-bayreuth.dehttps://www.polymer-engineering.de/

Funding information
Bayerisches Staatsministerium für Wissenschaft und Kunst, Grant/Award Number: F.2-M7426.10.2.1/4/16; Deutsche Forschungsgemeinschaft, Grant/Award Number: AL474/45-1

Abstract

In the realm of material characterization, the mechanical properties of polymer foams play a pivotal role in shaping their applicability across diverse industries. In this pursuit, we present a novel approach to standardize and automate the assessment of key mechanical parameters for Expanded Polypropylene (EPP) foams using a self-developed Python script, made freely available for the scientific community. We precisely determine the compression modulus, plateau onset, and onset of densification strain for EPP foams across various densities. The script's effectiveness is demonstrated through comparisons with manual evaluations and established standards, highlighting its superiority, consistency, and suitability for a wide range of materials and conditions. Moreover, the script enables the analysis of energy absorption, shedding light on the intricate relationship between density and energy dissipation. Finally, our approach was extended to other foams to provide insight on their mechanical properties. The automated methodology ensures accuracy, reproducibility, and efficiency, thereby advancing the understanding of foam materials and facilitating informed design decisions. This research contributes to laying a foundation for the standardized assessment of foam mechanical properties, which could potentially facilitate their effective use in other applications.

KEYWORDS

automated evaluation, mechanical properties of foams, mechanical testing, polymer foams

1 | INTRODUCTION

Polymer foams find extensive applications in various fields, ranging from thermal and acoustic insulation to packaging and cushioning materials. The exceptional combination of unique properties and their high potential for lightweight construction have positioned polymer foams as a significant market, with a global market share valued at 128 billion dollars in 2022.[1] In any application, ensuring sufficient mechanical performance is crucial. Particularly for foams used in protective equipment like helmets, the mechanical properties can be life-saving.[2,3] Hence, it is imperative to have a reliable and accurate assessment of the deformation behavior of polymer foams, ensuring reproducibility and precision.

One commonly employed method for assessing the mechanical performance of foams is the compression

Rodrigo Q. Albuquerque and Johannes Meuchelboeck contributed equally to this work.

test. This technique involves subjecting a foam sample to a compressive force and analyzing its response. Typically, the compression test involves gradually applying force to the foam sample at a constant rate, while simultaneously measuring the corresponding displacement and applied force. These measurements enable the derivation of various mechanical properties of the foam, including compressive strength, stiffness, and energy absorption capacity. Furthermore, the stress–strain curve obtained during the compression test offers insights into the foam's deformation and failure mechanisms. Compression testing is widely utilized in the foam industry to quantitatively evaluate crucial foam properties such as stiffness, impact absorption, and damping. Nevertheless, accurately evaluating stress–strain curves remains a daunting and time-consuming task. Often, manual evaluation becomes necessary, leading to compromised data quality.

Ashby et al. differentiate in general between foams with brittle, plastic–elastic and elastic deformation. The compression behavior of a foam is influenced by the material the foam is made of, the cellular structure, and the relative density.[4] Figure 1 illustrates a typical compressive stress–strain curve of an elastomeric polymer foam, based on the renowned research conducted by Gibson and Ashby.[5] The curve showcases the three distinct deformation regimes commonly observed: linear-elastic (I), plateau (II), and densification (III).

The compression modulus or elastic modulus (E_C) is the main parameter characterizing the linear-elastic regime (region I in Figure 1) and is defined as the slope of the linear region in the stress–strain curve. The compression modulus is widely used in the literature to compare the linear elastic behavior of bead foams.[2,3,6–12] However, an accurate automatic determination of E_C has not been established, and therefore values for the same foam and conditions may vary depending on the laboratory where it was measured or even the person doing the manual determination of E_C. For instance, for expanded polypropylene (EPP) foam with a density of 60 kg m^{-3} at room temperature, some reported values of E_C (in MPa) include 3.34,[11] 7.35,[6] and 8.34.[12] Among other problems, the *manual* determination of the maximum slope in the linear-elastic regime is prone to errors.

Another important mechanical parameter which can be obtained from stress–strain curves is the plateau stress (σ_{pl}, transition between regions I and II in Figure 1), which marks the transition point to the plateau regime, where irreversible deformation starts to occur.[5] Although there are no standardized methods to evaluate this property, it is commonly used in the literature to compare the mechanical performance of bead foams. Therefore, different methods are used to determine the plateau stress. One method is to calculate the property as the intersection between the slope of the linear elastic regime and the plateau regime[4,14,15] (Figure 2A). Andena et al.[6] determined the plateau stress at a fixed strain that is within the plateau range of the materials they compared. In particular, for foamed metals, the determination of the plateau stress with a very small (>0.2%) parallel shift of the slope of the linear elastic range is a commonly used

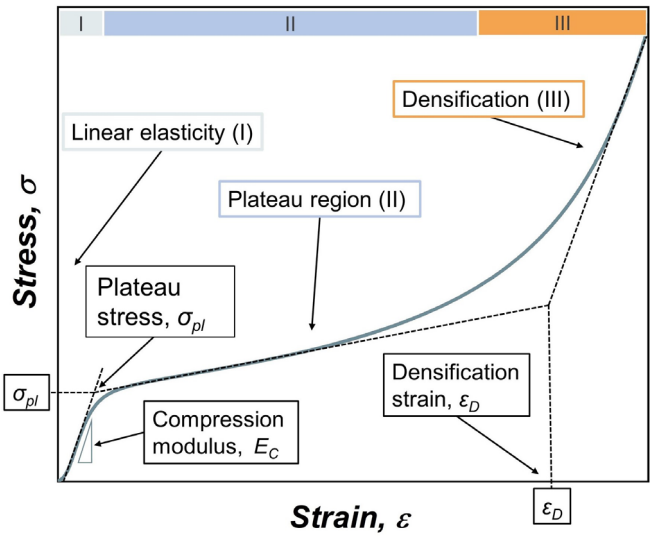

FIGURE 1 Typical compressive stress–strain curve of an elastomeric polymer foam with the three deformation regimes: linear-elastic (I), plateau (II), and densification (III). The most important parameters, like compression modulus (E_C), plateau stress (σ_{pl}) and densification strain (ϵ_D) are also shown.

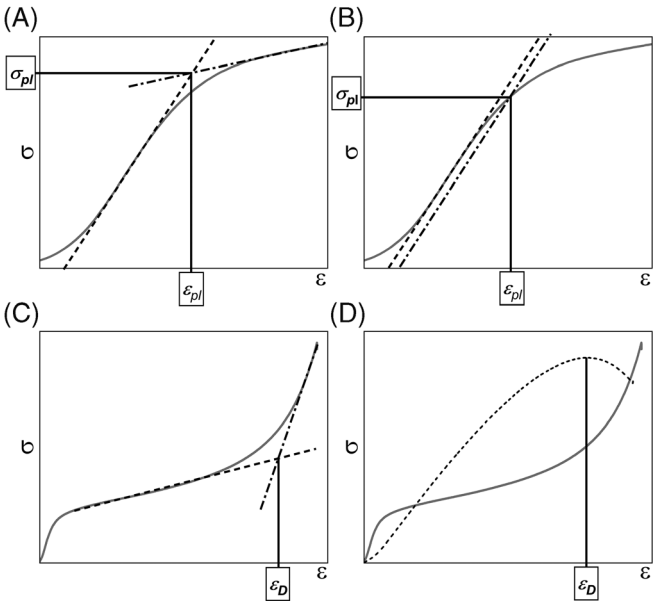

FIGURE 2 Different methods for calculating plateau onset (ϵ_{pl}, σ_{pl}) and the densification strain (ϵ_D) based on (A) the cross-sectional analysis of tangents,[5] (B) the shift of the tangent in the linear region,[13] (C) the crossing point between the plateau and densification tangents,[5] and (D) the maximum of the energy absorption efficiency.[13]

method[16,17] (Figure 2B). However, this method requires an accurate evaluation of the linear regime. Since there is no standardized method for polymer bead foams, different values of σ_{pl} have been reported for the same material and conditions. For example, for EPP with a density of about 30 kg/m^3, values of 0.17,[6] 0.15,[14] and 0.081 MPa[15] have been reported for the plateau stress.

A major advantage of polymer foams is their ability to absorb energy with only a small increase in stress (Figure 1) over a long period of compression.[18] The absorbed energy up to a certain strain can be calculated from the area under the compressive stress–strain curve. The efficiency of energy absorption is defined by Miltz et al. to evaluate the ability of a foam to absorb energy up to a given compression.[19] Often, the onset of densification is used as a limit for calculating energy absorption and comparing the density dependence of foams.[2,8,20]

The onset of densification (ϵ_D, transition between regions II and III in Figure 1) marks the end of the plateau regime and the beginning of the densification regime.[4] It can be determined by the crossing point between the tangent passing at the end of the stress–strain curve and the X axis of the curve (or zero stress), as shown in Figure 2C. The challenges of this method were discussed in the work of Basit and Cheon,[21] which led to the establishment of a densification range for polyurethane foam analysis. To avoid this uncertainty, Li et al.[13] introduced another method to determine the onset of densification using the maximum efficiency of energy absorption (Figure 2D).

Due to the wide range of reported values of mechanical properties for the same materials and conditions, it is necessary and crucial to standardize their evaluation. This study aims to accomplish this by developing a single Python script that automatically calculates all the mechanical properties discussed above in a unified, precise, and reproducible way, with free access to the scientific community. We also compare the results of the automated evaluation of mechanical properties with manual evaluations. To demonstrate the potential of automated analysis, we perform a comprehensive comparison of the mechanical properties of the widely used bead foams expanded polystyrene (EPS), expanded polypropylene (EPP), and expanded thermoplastic polyurethane (ETPU). In addition, by using a wide range of densities, we provide valuable insights into the density dependent energy absorption behavior.

2 | MATERIALS AND METHODS

2.1 | Experimental trials

The experimental trials were performed on a universal testing machine (Zwick/Roell Z010, Ulm, Germany). The displacement was determined by the traverse of the machine and the force was determined with an appropriate force cell. The materials used in this study were commercially available beads that were fused by the steam-chest molding process to form plates. The process parameters recommended in the accompanying data sheets were followed. Three samples per density of EPP (BASF SE, Ludwigshafen, Germany) and EPS (Sunpor Kunststoff, GmbH, St. Pölten, Austria) were tested according to DIN EN ISO 844 with skin. The samples were cut with a band saw to cuboids with a dimension of $50 \times 50 \times 40$ mm^3 for EPP and $50 \times 50 \times 20$ mm^3 for EPS. Six samples per density of ETPU (BASF SE, Ludwigshafen, Germany) were tested as a flexible foam with skin according to DIN EN ISO 3386-1. The cylindrical specimens were prepared with a water cutting unit with a diameter of 60 mm and a height of 20 mm.

After sample preparation, inhomogeneities in the material were tackled in the following way. (i) Parallel surfaces: The parallel tolerance of 1% was adopted according to DIN EN ISO 844 by measuring the height at three different positions per sample; (ii) Density inhomogeneity: The density of each sample was determined, and only samples with densities within small standard deviations were taken for testing. The mean values and corresponding standard deviation of the tested samples are shown in the third column of Table 1. The density ρ of every sample was calculated by $\rho = m/V$, where m and V are the mass and volume of the sample, respectively.

Due to different resistance against deformation, different force cells were used. The tested materials are listed in Table 1, together with their commercial name, average sample density and force cell.

The generated data were used to analyze the compression modulus, the onset of the plateau region and the densification strain. Our automatic approach of the evaluation of the compression modulus by the Python script was compared with calculating the slope between a fixed strain of 0.025% and 0.25% according to DIN EN ISO 604 and visually determining the most linear region following DIN EN ISO 844, which is a widely used standard for polymer foams.

In addition, the plateau onset and the densification strain were compared using the methods shown in Figure 2.

2.2 | Calculation of mechanical properties

The calculation of different mechanical properties was done using a self-written Python script, which is available as a Jupyter Notebook file (Supporting Information S1), where a link to a Panopto video with a tutorial showing how to use the script is also available. The stress–strain

TABLE 1 Overview of the studied samples.

Series name	Materials	Density (kg/m^3)	Force cell (kN)
EPS_30	A245 SE	32 ± 1	10
EPS_72	A245 SE	72 ± 1	50
EPP_30	Neopolen P8225	30 ± 0.1	50
EPP_60	Neopolen P9230K	60 ± 0.5	50
EPP_82	Neopolen P9280	82 ± 0.9	50
EPP_140	Neopolen P92HD105	140 ± 0.8	50
EPP_199	Neopolen P92HD130	199 ± 0.9	50
EPP_275	Neopolen P92HD180	275 ± 4	50
ETPU_244	Infinergy 32-100 U10	244 ± 2	20
ETPU_267	Infinergy 32-100 U10	267 ± 3	20
ETPU_296	Infinergy 32-100 U10	296 ± 6	20

curves available as an Excel file (.xlsx extension) and generated by the TestXpert II (Zwick GmbH) were directly used without further manual changes in the file. The most important steps to generate the mechanical properties from the stress–strain curves are shown in the pseudo code described in Algorithm 1.

After importing the Excel file (line 1), the values of ϵ and σ are checked to prevent negative values of σ, as well as repeated values of ϵ, which can cause problems in the evaluation of derivatives in the next step. For the calculation of the compression modulus, the derivative shown in line 4 is calculated to find the first peak in the derivative, starting from small ϵ values, which corresponds to the parameter ϵ_{max}. The slope of the tangent to the stress–strain curve at ϵ_{max} is the compression modulus (E_C, line 5). This tangent line is then shifted to the right along the $+\epsilon$ direction by 0.2 percentual points and defined as tangent' (line 6). The crossing point between this new tangent line and the stress–strain curve is defined as the end of the elastic region, also called the plateau onset (ϵ_{pl}, σ_{pl}, line 7), which defines the starting of the plateau region.

The calculation of the densification strain starts in line 10 of Algorithm 1, where the efficiency of compression (η) is calculated for each single value of ϵ available in the stress–strain curve. The integral used to calculate η shown in line 10 has been reported by Li et al.[13] The densification strain is then calculated as the ϵ value corresponding to the maximum value of $\eta(\epsilon)$, as shown in line 11. Having calculated ϵ_D and ϵ_{pl}, the simple integral shown in line 14 can be used to calculate the work of compression for the investigated material. The slope of the best linear fit to the plateau region is also calculated.

Algorithm 1 Calculating the mechanical properties of foams.

1: Import the Excel file.
2: Curate ϵ, σ values: $\sigma \geq 0$ and $\epsilon \rightarrow$ unique.
3: **procedure** COMPRESSION MODULUS (E_C), PLATEAU ONSET (ϵ_{pl}, σ_{pl}).
4: First peak of $d\sigma/d\epsilon : \epsilon_{max}$.
5: Slope of tangent at $\epsilon_{max} : E_C$.
6: Shift the tangent by 0.2% along the ϵ axis: tangent'.
7: Intersection of tangent' and curve: (ϵ_{pl}, σ_{pl}).
8: **end procedure**.
9: **procedure** ONSET OF DENSIFICATION STRAIN (ϵ_D).
10: Efficiency of energy absorption: $\eta(\epsilon) = \frac{\int_0^{\epsilon} \sigma(\epsilon')d\epsilon'}{\sigma(\epsilon)}$
11: $Argmax_{\epsilon}(\eta) : \epsilon_D$
12: **end procedure**.
13: **procedure** Energy absorption W_{comp}
14: $W_C = \int_{\epsilon_{pl}}^{\epsilon_D} \sigma(\epsilon) d\epsilon$
15: **end procedure**.

3 | RESULTS AND DISCUSSION

Figure 3 illustrates a typical output generated by the Python script, which not only generates txt files containing the data points used in all plotted curves, but also calculates several mechanical properties, as detailed below.

Compression modulus (E_C): The compression modulus is calculated from the derivative of the blue input curve, $d\sigma/d\epsilon$ (gray line in the top panel of Figure 3). The linear region used to determine the compression modulus is also plotted with higher magnification in the lower panel of Figure 3, from where it is possible to judge the goodness of the fit.

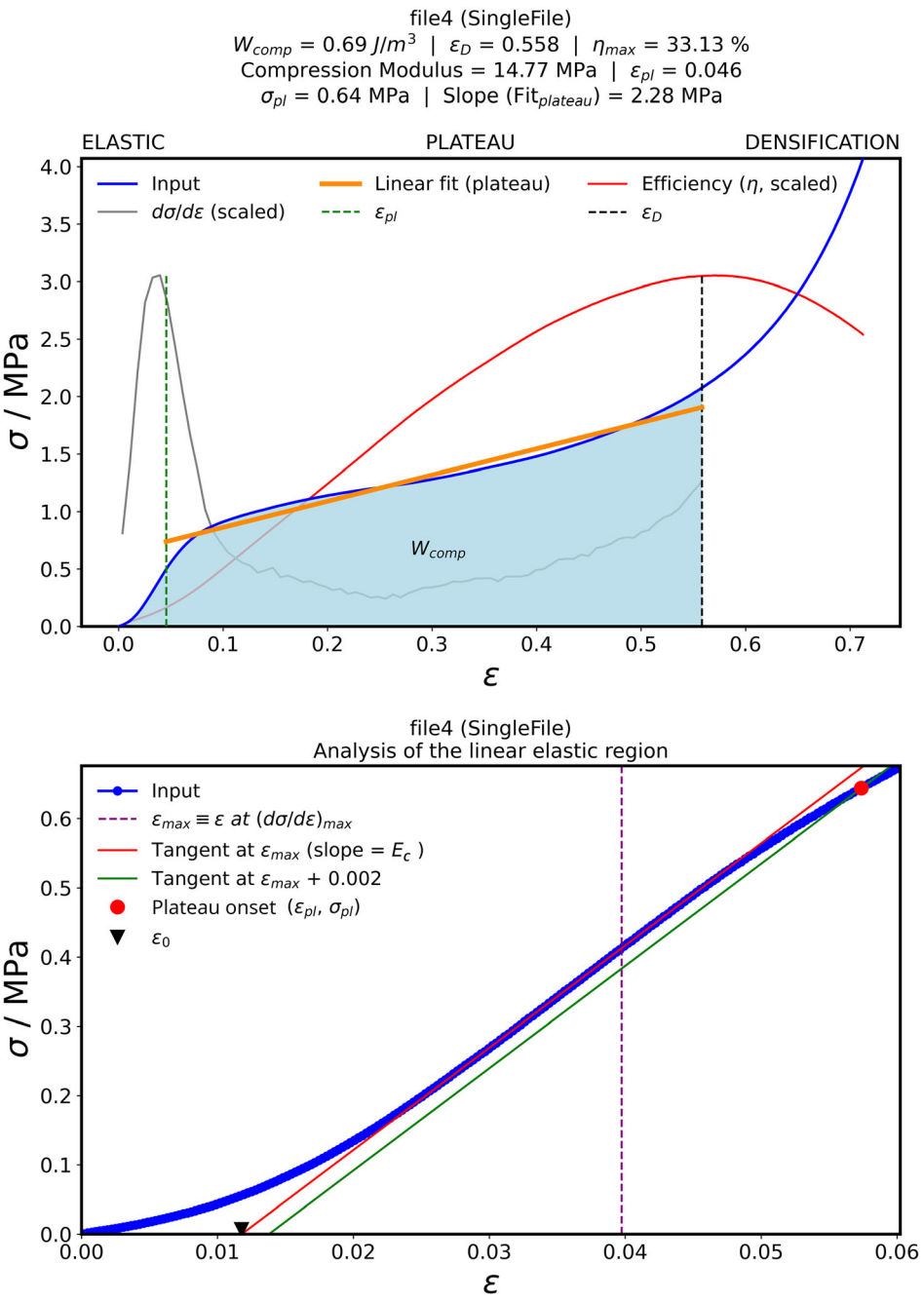

FIGURE 3 Partial output generated by the Python script. The elastic region shown in the upper subplot (region before the green dashed line) is shown with a larger magnification in the lower subplot.

Plateau onset (ϵ_{pl}, σ_{pl}): The plateau onset is calculated by first shifting the red tangent line shown in Figure 3 (bottom) to the right by 0.002 (or 0.2%), to generate the green line shown in the same subplot. The crossing point between the green line and the blue input curve defines the plateau onset (red circle), which has the coordinates plateau strain (ϵ_{pl}) and plateau stress (σ_{pl}), also provided in the title of the upper subplot. ϵ_{pl} is also represented by a green dashed vertical line in the top panel of Figure 3.

Onset of densification strain: The onset of densification strain is calculated with the maximum of the efficiency of energy absorption. In the top panel of Figure 3, the red curve represents the efficiency of compression (η), calculated as shown in line 10 of Algorithm 1 according to Li et al.[13] The maximum efficiency corresponds to the beginning of the densification region (indicated by the black dashed line) at a value of ϵ called densification strain (ϵ_D). The light blue region in the upper plot represents the area under the stress–strain (input) curve within the range of ϵ from 0 to ϵ_D. This area defines the work of compression, which is also calculated by the script.

Plateau region: The region between the plateau onset and the densification strain is called plateau region, and the slope of the best linear fit to that region (orange line in the upper subplot) is also calculated by the script.

The properties ϵ_{pl} and ϵ_D that are output by the script are calculated taking into account that ϵ starts to be

counted from the intersection between the tangent of the linear elastic region and the horizontal axis in the stress–strain input curve. This new zero in the horizontal (ϵ) axis is denominated ϵ_0 in the lower panel of Figure 3 and represented by a black triangle. This procedure allows for an easier comparison between stress–strain curves associated to different materials and experimental conditions.

The script was utilized to determine the mechanical properties of various EPP foams. These values were then compared to those obtained through manual evaluations following the DIN-ISO 604 and 844 standards. The calculated compression modulus, plateau onset and densification strain values for EPP at different densities are depicted in Figure 4.

According to the literature, the compression moduli reported for EPP were 2.34 ± 1.5 MPa (density of 30 kg/m^3) and 6.34 ± 2.16 MPa (density of 60 kg/m^3).[6,9,11,12] Despite variations in the base material and processing conditions, the calculated values from the script fall within this range, as shown in Figure 4.

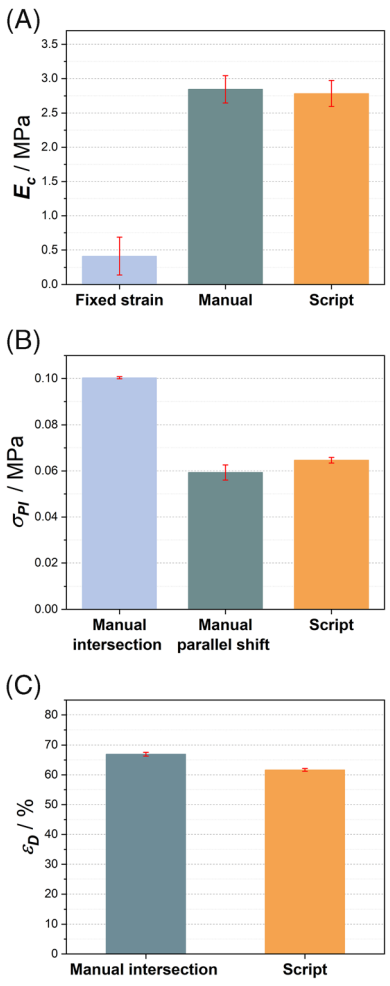

FIGURE 4 Comparison of various methods for determining (A) the compression modulus E_C, (B) plateau stress σ_{pl}, and (C) densification strain ϵ_D for EPP with a density of 30 kg/m^3. Error bars represent ± 1 standard deviation for three evaluations.

The compression modulus calculated manually and evaluated via the script were in excellent agreement with each other, as shown in Figure 4A (green and orange bars). The computation of the same property via a fixed strain is by definition different, as indeed shown in Figure 4A (gray bar) since it depends on the ranges adopted for ϵ (here, $\epsilon = 0.025$–0.25%).

For determining the plateau onset (Figure 4B), two distinct methodologies were employed: the intersection method (Figure 2A) and the parallel shift method (Figure 2B). The values obtained through computational analysis exhibited a comparable order of magnitude to those acquired via the manual parallel shift method (Figure 4B). However, it is noteworthy that these two values consistently registered as being lower than those derived using the manual intersection method. Such disparities, however, are anticipated due to the fundamentally dissimilar nature of these approaches (Figure 2A,B). Determining the onset of plasticity, defined as the first plastic deformation over the entire specimen, may require more sensitive techniques such as dynamic mechanical analysis (DMA). However, analysis of compressive stress–strain curves to obtain an estimate of the start of the plateau regime, defined here as "plateau onset", can be reliably calculated using the parallel displacement method and used to compare the mechanical response of bead foams.

In the existing literature, the plateau stress for EPP with a density of 30 kg/m^3 was documented as 0.13 ± 0.035 MPa, while EPP with a density of 60 kg/m^3 was characterized by an onset of 0.31 ± 0.064 MPa.[6,8,14,15] The relatively diminished values acquired in our investigation can be attributed to the distinct methodologies employed. Notably, the intersection method has a tendency to overestimate the linear elastic region, and further, the determination of the plateau onset is highly contingent upon the selected tangents, as elaborated upon earlier. The present study demonstrates that this challenge can be effectively addressed by adopting the parallel displacement method, as outlined in the established ISO 13314:2011 standards for metal foams. Utilizing the slope of the most linear elastic segment automatically identified by the computational script, which enables precise parallel displacement, yields a more precise determination of the plateau stress.[17]

Figure 4C presents a comparison between the manual intersection method (Figure 2C) and the computation of densification strain using the point of maximum energy absorption efficiency (Figure 2D). Evaluating the onset of densification strain by identifying the crossing point between the plateau and densification tangents results in

slightly elevated values in contrast to the efficiency-driven approach. Much like the assessment of the plateau onset via tangent intersection, determining the onset of densification strain is also susceptible to inherent errors. In a study by Basit et al., it was highlighted that the intersection method lacks precision and heavily relies on the user's choice of tangent line. Consequently, the authors introduced a range of densification instead of a single densification strain.[21] To mitigate this limitation, an alternate approach for determining densification strain was introduced by Li et al.,[13] based on maximizing energy absorption efficiency (Figure 4D). This method offers the potential to yield a more comparable value for densification strain. Therefore, the latter method (Figure 4D) has been incorporated into the computational script for enhanced accuracy.

We applied the described methodology to analyze the mechanical characteristics of the tested materials, as outlined in Table 1. Additionally, we present exemplary compressive stress–strain curves for EPS, EPP, and ETPU, with the results depicted in Figure 5.

Figure 5A highlights the distinct deformation behaviors of EPS and EPP with a density of 30 kg/m^3, as well as ETPU with a density of 267 kg/m^3, chosen as representative examples from the group of three materials. The observed dissimilarity in compression behavior can be

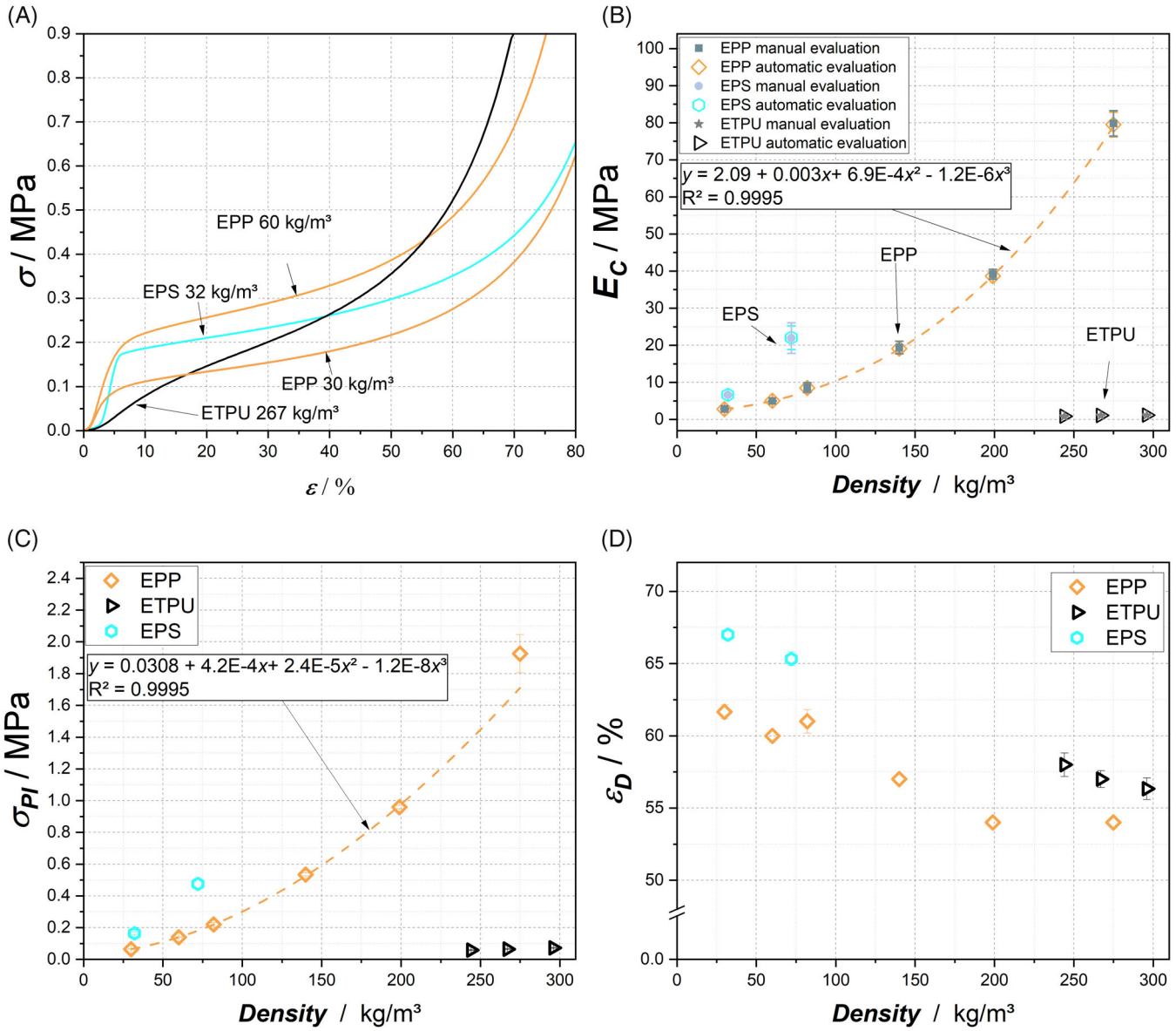

FIGURE 5 Comparison of the different dense EPS, EPP and ETPU bead foams in (A) representative stress–strain curves, in (B) comparison of the manual and automatic calculated compression modulus E_C, in (C) the plateau stress σ_{pl} and in (D) the analyzed onset of densification strain ϵ_D.

attributed to the influence of the underlying base material.[5] Notably, the EPS curve exhibits a clearly visible transition point demarcating the shift from linear elastic to plateau regions. While the stress–strain curves for EPP with 30 and 60 kg/m^3 densities exhibit similarities, the higher density variant demonstrates heightened resistance to deformation, effectively showcasing the dependence of foam mechanical properties on density. The transition point between the elastic and plateau regions in these curves is gradual and challenging to ascertain through visual inspection alone. In contrast, the ETPU curve, despite being associated with the highest density, displays the lowest resistance to deformation at the initial stages of the curve. It is worth noting that the slope of the ETPU curve remains comparable to that of the other two materials until significant deformation is reached. These traits collectively represent characteristic behaviors of an elastic foam and underscore the exceptional recovery behavior inherent in ETPU.[22]

Figure 5B illustrates the comparison between manual and automated evaluations of compression modulus. Notably, both methods yield similar values, regardless of the material and density, demonstrating the script's applicability across diverse materials. The distinct shapes of the compression curves contribute to varying mechanical properties (see Figure 5B–D). Specifically, when comparing EPS to EPP at 30 and 60 kg/m^3, EPS displays higher compression modulus and plateau stress, alongside higher densification strain. In contrast, among the three materials, ETPU exhibits the softest behavior, characterized by lower compression modulus and plateau strain. Even at a density exceeding 200 kg/m^3, ETPU retains these properties. Additionally, ETPU with a density of 267 kg/m^3 exhibits a higher onset of densification compared to EPP with a density of 275 kg/m^3.

Additionally, we conducted an analysis of energy absorption efficiency and energy absorption using the script, with the findings presented in Figure 6. Notably, EPS with a density of 30 kg/m^3 demonstrates the highest calculated energy absorption efficiency (Figure 6A). This is attributed to its rather brittle behavior, which contrasts with the behavior of EPP and ETPU. In the case of EPS, deformation leads to the irreversible crushing of cell walls and struts.[2] For EPS with higher densities, densification initiates at an earlier stage, consequently leading to a decrease in efficiency. For EPP, there is a peak at 90 kg/m^3, followed by a decrease at higher densities. Conversely, ETPU, characterized by its elastic behavior, exhibits the lowest energy absorption efficiency. In this material, energy is stored during loading and subsequently released during unloading, resulting in diminished energy absorption efficiency.

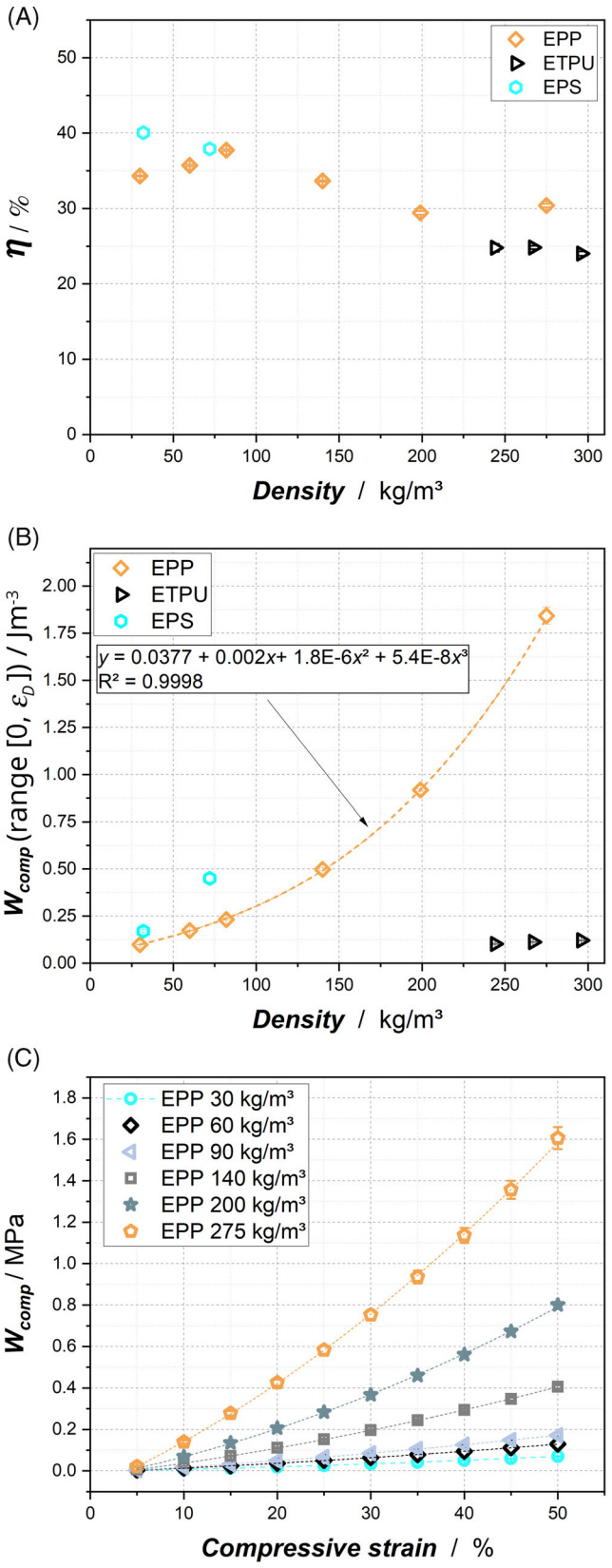

FIGURE 6 (A) Comparative analysis of energy absorption efficiency among EPS, EPP, and ETPU. In (B), visualization of energy absorption until the onset of densification. In (C), calculation of energy absorption across various upper limits of compressive strain for EPP over a density range spanning from 30 to 275 kg/m^3.

TABLE 2 Optimized parameters for the fittings shown in Figures 5 and 6.

Parameter	Intercept	B_1	B_2	B_3	R^2
Compression modulus	2.09	0.003	6.9E−4	1.2E−6	0.9995
Plateau onset	0.0308	4.2E−4	2.4E−5	−1.2E−8	0.9995
W_{comp} to ϵ_D	0.0377	0.002	1.8E−6	5.4E−8	0.9998

Figure 6B offers a visual representation of the intricate relationship between energy absorption and the initiation of densification. Notably, augmented density aligns with escalated energy absorption. Particularly noteworthy is the remarkable disparity between EPS and EPP, with EPS showcasing significantly superior energy absorption characteristics. In contrast, ETPU, owing to its intrinsic elastic behavior,[22] exhibits the least energy absorption among the three materials. Moreover, Figure 6C elucidates the density-dependent behavior of energy absorption concerning compressive strain. As compressive strain amplifies, so does energy absorption in tandem. This interrelation bears consequential implications for the design of components, underscoring the potential of high-density materials to achieve heightened energy absorption capacities.

The results of the different dense EPP show a clear density dependence of the compressive modulus, onset of plasticity (5) and energy absorption (6). All values can be fitted by a cubic fit with Equation (1). The power law fit was slightly worse (see the Supporting Information S1).

$$y = Intercept + B_1 x + B_2 x^2 + B_3 x^3 \quad (1)$$

The specific fit values for the investigated parameters are listed in Table 2.

4 | CONCLUSIONS

This study employed a comprehensive computational approach to analyze the mechanical properties of various EPP foams. The methodology not only generated graphical representations of mechanical behavior but also calculated critical parameters crucial for material characterization.

The compression modulus was accurately determined using the derivative of the stress–strain curve. This approach exhibited excellent agreement with manually obtained values and aligned well with literature-reported compression moduli for EPP at different densities. The technique's reliability was showcased by its ability to capture the varying deformation behaviors of distinct materials and densities.

The plateau onset and the onset of densification strain were calculated with precision by the script, comparing favorably to manual evaluations. The distinct methodologies used for determination were validated against established standards, highlighting the superiority of the proposed parallel shift method over traditional intersection techniques. This advancement was essential for achieving accurate and consistent results across varying materials and conditions.

Energy absorption efficiency and energy absorption were explored, shedding light on the impact of density on these parameters. Notably, EPS demonstrated exceptional energy absorption characteristics, primarily attributed to its rather brittle nature, while ETPU displayed the least energy absorption due to its inherent elasticity. The density-dependent behavior of energy absorption and its correlation with compressive strain highlighted the potential of high-density materials for enhanced energy absorption capabilities.

Furthermore, the study established cubic fits to represent the density-dependent trends of compression modulus, plateau onset, and energy absorption, providing concise mathematical expressions to model these behaviors accurately.

In summary, this computational approach offers a reliable and efficient means to assess the mechanical properties of EPP foams, providing insights into the interplay of density, mechanical behavior, and energy absorption. The methodology's precision and reliability can potentially help guide material selection and component design for other similar applications. The study's findings provide some insights into foam behavior and offer a direction for future research and practical use of foam materials.

ACKNOWLEDGMENTS

This publication received funding from the University of Bayreuth through the Open Access Publishing funding program. Portions of this research were also supported by the "Bayerischen Staatsministerium für Wissenschaft und Kunst" under grant number F.2-M7426.10.2.1/4/16 in Germany, as well as by the DFG project number 437872031 (AL474/45-1). We extend our sincere gratitude for the financial support provided. Open Access funding enabled and organized by Projekt DEAL.

ORCID

Holger Ruckdäschel https://orcid.org/0000-0001-5985-2628

REFERENCES

[1] Grand View Research, Market analysis report: Polymer foam market size, share & trends analysis report by type (polystyrene, polyurethane, polyolefin, melamine, phenolic, pvc), by application, by region, and segment forecasts, 2022–2030.

[2] L. Di Landro, G. Sala, D. Olivieri, *Polym. Test.* **2002**, *21*, 217.

[3] A. Krundaeva, G. de Bruyne, F. Gagliardi, W. van Paepegem, *Polym. Test.* **2016**, *55*, 61.

[4] M. F. Ashby, *Philos. Trans. R. Soc., A* **2006**, *364*, 15.

[5] L. J. Gibson, M. F. Ashby, *Cellular Solids: Structure and Properties*, 2nd ed., Cambridge University Press, Cambridge **2014**.

[6] L. Andena, F. Caimmi, L. Leonardi, M. Nacucchi, F. de Pascalis, *J. Cell. Plast.* **2019**, *55*, 49.

[7] I. Beverte, *J. Cell. Plast.* **2004**, *40*, 191.

[8] A. Reyes, T. Børvik, *Mater. Today Commun.* **2018**, *17*, 541.

[9] P. Rumianek, T. Dobosz, R. Nowak, P. Dziewit, A. Aromiński, *Materials (Basel, Switzerland)* **2021**, *14*, 249.

[10] N. Weingart, D. Raps, J. Kuhnigk, A. Klein, V. Altstädt, *Polymer* **2020**, *12*, 2314.

[11] A. Himmelsbach, T. Standau, J. Meuchelböck, V. Altstädt, H. Ruckdäschel, *J. Polym. Eng.* **2022**, *42*, 277.

[12] F. A. O. Fernandes, R. T. Jardin, A. B. Pereira, R. J. Alves de Sousa, *Mater. Des.* **2015**, *82*, 335.

[13] Q. M. Li, I. Magkiriadis, J. J. Harrigan, *J. Cell. Plast.* **2006**, *42*, 371.

[14] R. Bouix, P. Viot, J. L. Lataillade, *Int. J. Impact Eng.* **2009**, *36*, 329.

[15] D. T. Morton, A. Reyes, A. H. Clausen, O. S. Hopperstad, *Mater. Today Commun.* **2020**, *23*, 100917.

[16] International Organization for Standardization, ISO 13314: 2011: Mechanical testing of metals—ductility testing—compression test for porous and cellular metals, 2011–2012.

[17] T. Mankovits, T. A. Varga, S. Manó, I. Kocsis, *J. Mech. Eng.* **2018**, *64*, 105.

[18] M. Avalle, G. Belingardi, R. Montanini, *Int. J. Impact Eng.* **2001**, *25*, 455.

[19] J. Miltz, O. Ramon, *Polym. Eng. Sci.* **1990**, *30*, 129.

[20] N. Du Uy, C. B. Lan, C. Bethke, J. Meuchelböck, T. Standau, V. Altstädt, H. Ruckdäschel, *Materials (Basel, Switzerland)* **2022**, *15*, 4205.

[21] M. M. Basit, S. S. Cheon, *Mech. Time-Depend. Mater.* **2019**, *23*, 207.

[22] C. Ge, Q. Ren, S. Wang, W. Zheng, W. Zhai, C. B. Park, *Chem. Eng. Sci.* **2017**, *174*, 337.

SUPPORTING INFORMATION

Additional supporting information can be found online in the Supporting Information section at the end of this article.

How to cite this article: R. Q. Albuquerque, J. Meuchelböck, H. Ruckdäschel, *J. Polym. Sci.* **2023**, 1. https://doi.org/10.1002/pol.20230704